AIP | Review of Scientific Instruments

New experimental platform to study high density laser-compressed mattera)

M. Gauthier, L. B. Fletcher, A. Ravasio, E. Galtier, E. J. Gamboa, E. Granados, J. B. Hastings, P. Heimann, H. J. Lee, B. Nagler, A. Schropp, A. Gleason, T. Döppner, S. LePape, T. Ma, A. Pak, M. J. MacDonald, S. Ali, B. Barbrel, R. Falcone, D. Kraus, Z. Chen, M. Mo, M. Wei, and S. H. Glenzer

Citation: Review of Scientific Instruments **85**, 11E616 (2014); doi: 10.1063/1.4896175
View online: http://dx.doi.org/10.1063/1.4896175
View Table of Contents: http://scitation.aip.org/content/aip/journal/rsi/85/11?ver=pdfcov
Published by the AIP Publishing

New experimental platform to study high density laser-compressed matter[a)]

M. Gauthier,[1,b)] L. B. Fletcher,[1] A. Ravasio,[1,2] E. Galtier,[1] E. J. Gamboa,[1] E. Granados,[1] J. B. Hastings,[1] P. Heimann,[1] H. J. Lee,[1] B. Nagler,[1] A. Schropp,[1] A. Gleason,[3] T. Döppner,[4] S. LePape,[4] T. Ma,[4] A. Pak,[4] M. J. MacDonald,[5] S. Ali,[6] B. Barbrel,[6] R. Falcone,[1] D. Kraus,[6] Z. Chen,[7] M. Mo,[7] M. Wei,[8] and S. H. Glenzer[1]
[1]*SLAC National Accelerator Laboratory, Menlo Park, California 94025, USA*
[2]*LULI, Ecole Polytechnique, Palaiseau, France*
[3]*Department of Geological and Environmental Sciences, Stanford University, Menlo Park, California 94025, USA*
[4]*Lawrence Livermore National Laboratory, P.O. Box 808, Livermore, California 94551, USA*
[5]*Atmospheric, Oceanic, and Space Science Department, University of Michigan, Ann Arbor, Michigan 48109, USA*
[6]*Physics Department, University of California Berkeley, Berkeley, California 94709, USA*
[7]*Physics Department, University of Alberta, Edmonton, Alberta T6G 2V4, Canada*
[8]*Inertial fusion technology Department, General Atomics, San Diego, California 85608, USA*

(Presented 4 June 2014; received 5 June 2014; accepted 6 September 2014; published online 26 September 2014)

We have developed a new experimental platform at the Linac Coherent Light Source (LCLS) which combines simultaneous angularly and spectrally resolved x-ray scattering measurements. This technique offers a new insights on the structural and thermodynamic properties of warm dense matter. The < 50 fs temporal duration of the x-ray pulse provides near instantaneous snapshots of the dynamics of the compression. We present a proof of principle experiment for this platform to characterize a shock-compressed plastic foil. We observe the disappearance of the plastic semi-crystal structure and the formation of a compressed liquid ion-ion correlation peak. The plasma parameters of shock-compressed plastic can be measured as well, but requires an averaging over a few tens of shots. [http://dx.doi.org/10.1063/1.4896175]

I. INTRODUCTION

The study of warm dense matter (WDM), i.e., high energy density, has gathered enormous scientific interest in various domains from inertial confinement fusion to planetary physics.[1]. Shock-compressed material undergoes solid-solid or solid-liquid phase transition, spanning a rich phase space of new structures and new material properties in which strong correlation and quantum effects play a major role. However, modeling such regime is very challenging and success relies on how accurately the matter can be characterized experimentally. Although optical diagnostics give access to macroscopic quantities of high-density system, they cannot provide any direct measurements of the microscopic structure, which is critical for studying phase transition. In contrast to optical beams, x-rays can penetrate high-density materials providing direct *in situ* measurements of their structure and properties. Taking advantage of the powerful collimated, high-energy x-rays delivered by the free electron laser (FEL) at LCLS, we have developed a unique experimental platform dedicated to study high-energy density matter. Our platform provides simultaneous measurements of angularly and spectrally resolved x-ray scattering of WDM. The lattice structure is revealed from the angle-resolved scattering to clearly identify phase-transitions.[2] The spectral measurements allow for characterization of plasma parameters such as electron density (n_e), temperature (T), electron-ion collision frequency, and degree of ionization.[3] These quantities can then be correlated with macroscopic properties measured by additional optical diagnostics such as shock velocity and reflectivity from VISAR (velocity interferometer system for any reflector)[4] and plasma thermal emission from SOP (streaked optical pyrometry).[5] In addition, the < 50 fs duration of the FEL pulse allows resolving the dynamic of the shock-induced phase transitions which occur on a ultrafast time scale. To illustrate the capabilities of our platform, we present results we obtained in an experiment to characterize the state of shock-compressed plastic foils.

II. EXPERIMENTAL PLATFORM

Our experimental platform applied to study compressed plastic is shown in Fig. 1. A 40 μm thick polypropylene (PP) target (density 0.885–0.94 g/cm^3) was irradiated by two counter-propagating laser pulses, each with a nominal energy of 6 J, 3 ns square pulse duration and 0.5 ns rise time. Each face of the foil was irradiated with 527 nm laser light at an intensity of 2×10^{13} W/cm^2 to launch two counter-propagating shocks. To ensure the planarity of the shocks, the beam profiles were smoothed with continuous phase plate to 60 μm diameter focal spots. The FEL beam was used as a probe for the experiments. It was focused to a 10 μm diameter spot, propagating coaxial to the optical lasers. FEL beam provided up to 0.6 mJ of x-rays with an energy of 8034 eV and relative spectral bandwidth of 2%. The delay between the optical laser and

[a)]Contributed paper, published as part of the Proceedings of the 20th Topical Conference on High-Temperature Plasma Diagnostics, Atlanta, Georgia, USA, June 2014.
[b)]maxence.gauthier@stanford.edu

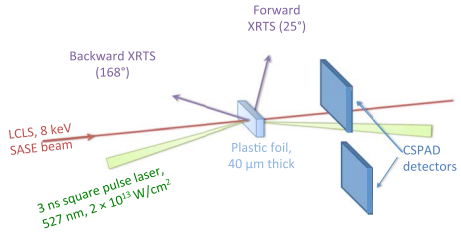

FIG. 1. Experimental set-up.

the x-ray FEL pulses can be varied to access to the dynamic of the compression process. The angularly resolved x-ray scattering were detected by two Cornell-SLAC Pixel Array Detectors (CSPADs).[6] The two CSPADs provided angular coverages of $2\theta = 17°–55°$ and 40°–60°, respectively. Two von-Hàmos x-ray Thomson scattering spectrometers were used to spectrally resolve the scattered radiation at 25° (F-XRTS) and 168° (B-XRTS). While F-XRTS measures collective properties of the plasma, B-XRTS measures non-collective and scattering over single particle.[3] The scattered x-rays were analyzed by cylindrically bent graphite crystal, Highly Annealed Pyrolytic Graphite (HAPG)[7] for FXRTS and Highly Oriented Pyrolytic Graphite (HOPG)[8] for BXRTS.

III. RESULTS

A. Angularly resolved x-ray scattering

Angularly resolved measurement of scattered x-rays provides information on the spatial correlations of the ionic structure. When probing crystals, incident x-rays reflects onto the highly ordered ion lattice and exhibits Debye-Scherrer diffraction rings. As shown in Figs. 2(a) and 2(b) for the PP sample corresponding to a partial alignments of the polymer molecular chains called lamellae.[10] The scattered signal is then concentrated at very specific angle position on intense Bragg peaks (see Fig. 2(e)). By looking at the angular positions of the diffraction rings, we are able to detect solid-solid shock-induced phase transition with a very good accuracy. This technique is also sensitive to solid-liquid phase transitions, identified by a loss of long-range correlations inducing a strong broadening and decrease of intensity of the scattered peaks. In this way, we observe the melting of PP sample, i.e., loss of the lamellar structure, from the strong heating induced by the shock (see Figs. 2(c), 2(d), and 2(f)). From 0.2 ns to 1.6 ns delay after the beginning of the compression, we clearly observe a progressive intensity decrease of the two main Bragg peaks. This is coincident with the appearance of a broad ion-ion correlation peak, shifting to lower scattering angle with time, which dominates at the later times. Although future experiments together with simultaneous measurements of the background are required for a quantitative determination of the density and structure factors, our diagnostic provides a direct access to the dynamics of the compression and heating of the sample.

In order to test the potential disruptive effect of x-ray self-heating on the sample, we irradiated the same spot on the PP with 50 x-ray pulses. As shown in Fig. 2(e), we notice a very good stability of the peak position and a variation below 20% of the different peak intensities. The heating caused by the probe beam does not induced any visible effect on the crystal structure of the sample.

B. Spectrally resolved x-ray scattering

Now that we have access to the ionic microstructure, the diagnostics based on spectrally resolved x-ray scattering helps to determine the conditions achieved by the compressed sample. In the forward geometry, i.e., at small scattered vector k, the scattering occurs on collective density fluctuations. The energy shift of the plasmon feature from the incident x-rays is used as a sensitive marker of the electron density, especially for low temperature high-density plasmas.[11] This shift can be modeled by the modified Bohm-Gross dispersion relation, $\omega_{pl}^2 = \omega_p^2 + 3k^2 v_{th}^2\ (1+0.088 n_e \Lambda_{th}^3) + (\hbar k^2/2m_e)^2$, where ω_p is the plasma frequency, v_{th} is the thermal velocity, and

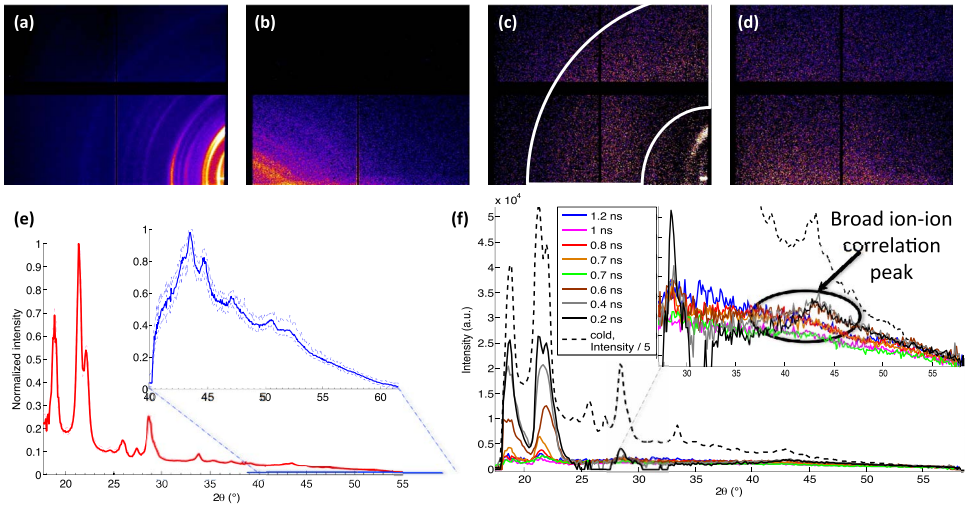

FIG. 2. X-rays scattered map detected on the CSPADs from non-compressed ((a) and (b)) and compressed ((c) and (d)) plastic; Angularly resolved lineout (averaged over the azimuth) recorded by the CSPADs from (e) cold plastic, the dotted lines corresponding to the maximum variations of the signal measured during 50 consecutive x-ray shots, and from (f) compressed plastic from 0 to 1.2 ns after the beginning of the compression.

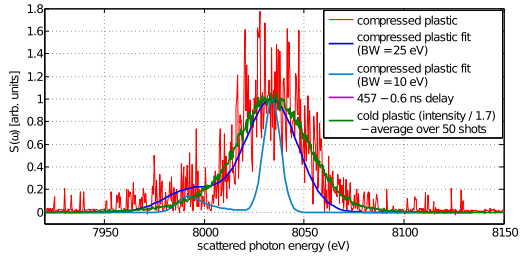

FIG. 3. Comparison of spectrally resolved F-XRTS spectra from cold (green) and compressed plastic (red) with theoretical dynamic structure factor calculations compute for an electron density of free electron of 5.2 $\times 10^{23}$cm^{-3} for 10 (light blue) and 30 eV (dark blue) incident x-ray spectral bandwidth (BW).

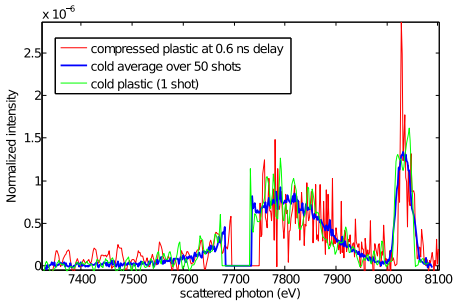

FIG. 4. Comparison of spectrally resolved B-XRTS spectra obtained in cold (green) and compressed plastic 0.6 ns after the beginning of the compression (red). The bold and dark blue line corresponds to the scattered signal in cold plastic averaged over 50 consecutive shots. The signal is normalized over the Compton peak area.

Λ_{th} is the thermal wavelength. This relation includes effects of the plasma frequency oscillation, of the thermal pressure, degeneracy effects from Fermi pressure and quantum shift.[3] For shock-compressed plastic 0.6 ns after the beginning of the compression (see Fig. 3), we observe in forward scattering ($k = 1.8$ Å^{-1}) a weak scattering feature downshifted by 42 eV with respect to the electron elastic peak centered at 8 keV that can be interpreted as a plasmon. According to a theoretical fit of the dynamic structure factor,[9] it would indicate an electron density of free electron of 5.2 $\times$ 10^{23}cm^{-3}. To better resolved this plasmon feature and increase the precision of the density measurements, future experiments would require averaging over few tens of shots for each time delay using the angularly resolved x-ray scattering signal to ensure the reproducibility. Note that reducing spectral width of the source would increase as well the resolution of the plasmon feature (see Fig. 3). We remark as well that the elastic peak is weaker in compressed plastic compared to cold plastic (the signal being normalized with respect to the energy measured in the FEL). This behavior, consequence of the disappearance of the Bragg peak located close to 25°, is in qualitative agreement with the angularly resolved measurements shown earlier (see Fig. 2(e)). In the backscatter geometry, the scattered vector k (here 8.1 Å^{-1}) is much larger to the plasma screening length. The scattering therefore occurs on single electrons and the spectrum shows a Compton peak, result of the scattering from free and weakly bound electrons. Its shape and width is then sensitive to the electron velocity distribution function and thus can provide information on the electron density and temperature.[3] For shock-compressed plastic 0.6 ns after the beginning of the compression (see Fig. 4), we observe a faint increase of the Compton width with respect to cold plastic. This can be interpreted as an increase of the electron density or/and temperature. However, due the poor signal to noise ratio added to the low temperature expected here, we cannot determine the electron temperature. As shown in Fig. 4 with cold plastic, averaging over tens shots can solve this issue. We note as well that the elastic peak shows a higher intensity in shock-compressed plastic than in cold plastic. This comportment is likely due to the broadening of the ion-ion correlation function at a wavenumber location where no Bragg peak is present in cold plastic. Theoretical modeling are required to further explain this behavior.

IV. CONCLUSION

We have presented a new experimental platform operated at LCLS that combines simultaneous angularly resolved and spectrally resolved x-ray scattering measurements to accurately characterize the state of WDM. Testing it on a shock-compressed plastic sample, we have observed the solid-liquid phase transition, as well as shown a way to estimate the electron density and temperature achieved at each time of the compression. We point out that for compressed plastic, a reliable and accurate measurement of these last parameters requires an averaging over a few tens of shots. With its unique combination of complementary diagnostics, our platform provides access to a very rich set of *in situ* physical quantities that makes it an ideal tool to characterize high-density matter and benchmark *ab initio* modeling.

ACKNOWLEDGMENTS

This work was performed at the Matter at Extreme Conditions (MEC) instrument of LCLS, supported by the DOE Office of Science, Fusion Energy Science under Contract No. SF00515. This work was supported by the DOE Office of Science, Fusion Energy Science under FWP 100182, by the Peter-Paul-Ewald Fellowship of the VolkswagenStiftung, and partially supported by DOE Office of Basic Energy Sciences, Materials Sciences and Engineering Division, under Contract No. DE-AC02-76SF00515. This work was performed under the assistance of the U.S. Department of Energy by Lawrence Livermore National Laboratory under Contract No. DE-AC52-07NA27344. The targets were supported by Laboratory Directed Research and Development.

[1]M. Ross *et al.*, Philos. Trans. R. Soc. London, Ser. A **303**, 303 (1981).
[2]D. Milathianaki *et al.*, Science **342**, 220–223 (2013).
[3]S. H. Glenzer and R. Redmer, Rev. Mod. Phys. **81**, 1625 (2009).
[4]L. Baker and R. Hollenbach, J. Appl. Phys. **43**, 4669 (1972).
[5]P. Celliers and A. Ng, Phys. Rev. E **47**, 3547 (1993).
[6]L. J. Koerner *et al.*, IEEE Trans. Nucl. Sci. **56**, 2835 (2008).
[7]U. Zastrau *et al.*, JINST **8**, P10006 (2013).
[8]U. Zastrau *et al.*, JINST **7**, P09015 (2012).
[9]R. Thiele *et al.*, Phys. Rev. E **78**, 026411 (2008).
[10]G. Natta and P. Corradini, Nuovo Cimento **15**, 40 (1960).
[11]A. Holl *et al.*, High Energy Density Phys. **3**, 120 (2007).